Modelling of Processes Involving Electromagnetic Phenomena

V. Robin[1], E. Feulvarch[1,2], J.M. Bergheau[2]

[1]*ESI France – ESI Group, Le Récamier, 70 Rue Robert, 69458 Lyon cedex 06, France*
URL: www.esi-group.com *e-mail: vincent.robin@esi-group.com*

[2]*Laboratoire de Tribologie et Dynamique des Systèmes, UMR 5513 CNRS/ECL/ENISE, Ecole Nationale d'Ingénieurs de Saint Etienne, 58 Rue Jean Parot, 42023 Saint Etienne cedex 02, France*
URL: ltds.ec-lyon.fr *e-mail: eric.feulvarch@enise.fr; bergheau@enise.fr.*

ABSTRACT: Induction phenomena are increasingly employed as industrial manufacturing processes because they exhibit many advantages besides the safety and tidiness of the working environment. Indeed, this kind of process is very appreciated because of its repeatability. As an example, we can compare induction heating with any other classical heat convective process: for heat-treatment, induction heating is much more accurate as the thickness of the workpiece to be treated can be electrically controlled. If we consider electro-magneto-forming (EMF also known as magnetic pulse forming) of tube or sheet metal which is deformed by applying a pressure generated by an intense transient magnetic field, the resulting strain rates reach higher values than during a stamping operation. EMF increases the formability limit of metal and is very efficient to achieve the end shape that is desired especially in sharp corner regions. This paper describes the numerical modelling of EMF process.

Key words: FEM, Numerical modelling, Electromagnetism, EMF

1 INTRODUCTION

Electromagnetic forming requires the generation of a high and transient magnetic field using an appropriate electrical device bringing energy of about hundreds of kJ [1]. This field is developed in the surrounding of the forming coil and the metallic object to be formed. Like any other forming process, a die might be necessary to give the workpiece the required final geometry. The high current pulse passing through the coil is producing eddy currents in the opposite direction to the process current that causes global Laplace's repulsive forces between the two components due to microscopic Lorentz's forces. Modelling such a forming process requires to couple multiphysical phenomena and their interaction as described in figure 1.

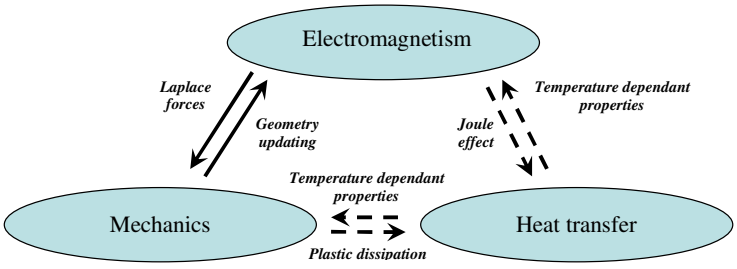

Fig. 1. Interaction between involved physical phenomena

The effect of temperature variations was considered negligible for the simulation of the stamping process. Indeed temperature effects are much localised. Eddy currents generate a high thermal power density in a very short time, so that temperatures remains quite low and heat transfer by conduction cannot affect the complete workpiece mechanical behaviour as shown in the last part of this paper. The plastic work is distributed in the whole plastically deformed part of the component and does not need to be considered more than for classical stamping process.

On the numerical modelling point of view, in addition to solve Maxwell's equations [2], the finite element (FE) software can also couple the strong interactions between electromagnetism, heat transfer and mechanical behaviour which drive induction processes [3, 4]. The first two parts of the paper present the numerical modelling of these physical phenomena. In case processes involve movable parts or workpiece compressed into a die, the meshing of the surrounding air makes FE method difficult to handle with because remeshing may be required to save the good quality of elements. The solution to get over this trouble and which consists in combining FE with boundary element method (BEM) is also described in the document. In the last part some examples of industrial applications for which the so developed code can be used for virtual testing are presented for validation. Finally

numerical results are compared with experiments on a 3D model highlighting the interest of numerical modelling for process improvements. This investigation was partly conducted within the framework of a European project called EMF (G3RD-CT-2002-00798) [5].

2 ELECTROMAGNETISM FINITE ELEMENT MODELLING

2.1 Maxwell's equations

The electromagnetism phenomena are governed by Maxwell's equations. For sinusoidal currents the frequency of which is of the order of 10^{12}Hz, displacement currents can be neglected and so the equations to be solved reduce to

$$curlH = J \tag{1}$$

$$curlE = -\frac{\partial B}{\partial t} \tag{2}$$

$$divB = 0 \tag{3}$$

where $\boldsymbol{H}$ is the magnetic field, $\boldsymbol{B}$ is the magnetic induction or magnetic flux density vector, $\boldsymbol{E}$ is the electric field and $\boldsymbol{J}$ is the current density.
Constitutive material behaviour laws relate these quantities together such as the magnetization law (4) and the Ohm's law (5).

$$B = \mu\left(\|H\|, \theta\right) \cdot \left(H\right) \tag{4}$$

where $\boldsymbol{\mu}$ is the magnetic permeability that can depend considerably on temperature (Curie point) and on $\|H\|$.

$$J = \sigma(\theta)E \tag{5}$$

where $\boldsymbol{\sigma}$ is the electric conductivity which depends on temperature.
In order to solve this system of equations, the magnetic vector potential $\boldsymbol{A}$ is introduced from equation (3)

$$B = curlA \tag{6}$$

To ensure the uniqueness of $\boldsymbol{A}$, a gauge condition (7) is mandatory (Coulomb's gauge):

$$divA = 0 \tag{7}$$

Equation (2) with relation (6) gives

$$E = -\frac{\partial A}{\partial t} - gradV \tag{8}$$

In equation (8), $\boldsymbol{E}$ is not uniquely defined because it depends on the electric scalar potential $\boldsymbol{V}$ that leads to introduce the conservation of current density (9) from equation (1).

$$div\left(J\right) = 0 \tag{9}$$

2.2 Partial differential problem

Finally the system of equations to be solved is the following:

$$\sigma\left(\frac{\partial A}{\partial t} + gradV\right) + curl\left(\nu\ curlA\right) = 0 \tag{10}$$

$$div\left(\sigma\left(\frac{\partial A}{\partial t} + gradV\right)\right) = 0 \tag{11}$$

$$divA = 0 \tag{12}$$

where $\upsilon = \frac{1}{\mu}$ is the magnetic reluctivity.
The different boundary conditions possible in a bounded domain Ω with boundary $\partial\Omega = \partial\Omega_A \cup \partial\Omega_H = \partial\Omega_V \cup \partial\Omega_j$ are:
Prescribed magnetic vector potential that can depends on time

$$A(\mathrm{t}) = A^d(\mathrm{t}) \text{ on } \partial\Omega_A \tag{13}$$

Prescribed electric potential

$$V(\mathrm{t}) = V^d(\mathrm{t}) \text{ on } \partial\Omega_V \tag{14}$$

Prescribed tangential magnetic field (with n is the outward unit normal to the surface)

$$H(\mathrm{t}) \times n = H^d(\mathrm{t}) \text{ on } \partial\Omega_H \tag{15}$$

Prescribed surface current density

$$-J \cdot n = \sigma\left(\frac{\partial A}{\partial t} + gradV\right) \cdot n = j^d \text{ on } \partial\Omega_j \tag{16}$$

2.3 Finite element formulation

The variational problem consists in finding $\boldsymbol{A}$ and $\boldsymbol{V}$ such as $\forall \mathbf{A}^*,\ \mathbf{A}^* = 0 \text{ on } \partial\Omega_{\mathbf{A}}$ and $\forall V^*, V^* = 0 \text{ on } \partial\Omega_V$:

$$\int_\Omega A^*.\sigma.\left(\frac{\partial A}{\partial t} + gradV\right)dv + \int_\Omega curlA^*.\nu.curlA\ dv + \alpha\int_\Omega divA^*.divA\ dv - \int_{\partial\Omega_{\mathbf{H}}} A^*.H^d\ ds = 0 \tag{17}$$

$$\int_\Omega gradV^*.\sigma.\left(\frac{\partial A}{\partial t}+gradV\right)dv-\int_{\partial\Omega_j}V^*.j^d\,ds=0 \quad (18)$$

This formulation leads to the following first order partial differential system of equations:

$$\begin{Bmatrix}\Psi_{\mathbf{A}}(\mathbf{A},V)\\ \Psi_V(\mathbf{A},V)\end{Bmatrix}=\begin{Bmatrix}\mathbf{R}_{\mathbf{A}}(\mathbf{A},V)\\ \mathbf{R}_V(\mathbf{A},V)\end{Bmatrix}-\begin{bmatrix}\mathbf{C}_{\mathbf{AA}} & 0\\ \mathbf{C}_{V\mathbf{A}} & 0\end{bmatrix}.\begin{Bmatrix}\dot{\mathbf{A}}\\ \dot{V}\end{Bmatrix}=\begin{Bmatrix}0\\ 0\end{Bmatrix} \quad (19)$$

Equations (19) are solved step by step in time using an implicit backward Euler method. At each time step the solution is obtained through a Newton-Raphson procedure.

2.4 Finite element method and boundary element method coupling

Air is an electromagnetic medium which must be included in the magnetodynamic modelling when using vector potential formulation. For convenience it is possible to use a method coupling finite elements in the conductive media and boundary elements for the surrounding air. The air has a linear behaviour and is a non-conductive medium. Therefore, considering equations (10) and (12), the problem to be solved in Ω_{BEM} reduces to (20):

$$\Delta A=0 \quad (20)$$

with boundary conditions:

- $A=0$ to infinity $\partial\Omega_\infty$,
- continuity of A and $divA$ on $\partial\Omega_{FEM\cap BEM}$ (as compatible meshes are used for Ω_{FEM} and $\partial\Omega_{FEM\cap BEM}$, this condition is naturally satisfied),
- $H\times n_{FEM}=H\times n_{BEM}$ on $\partial\Omega_{FEM\cap BEM}$.

Using a variationnal problem to set up the boundary element formulation, it can be shown that the boundary element method applied to the air leads to solve the following matrix system [4] where $\{\mathbf{A}_{BEM}\}$ is a subset of $\{\mathbf{A}\}$ limited to the nodes belonging to $\partial\Omega_{FEM\cap BEM}$:

$$[\mathbf{H}].\{\mathbf{A}_{BEM}\}=[\mathbf{G}].\{\mathbf{H}_{BEM}\} \quad (21)$$

Let us call $[\mathbf{T}].\{\mathbf{H}_{BEM}\}$ the part of $\mathbf{R}_{\mathbf{A}}(\mathbf{A},V)$ concerning the conditions on $\partial\Omega_{FEM}$.

Finally, it appears that matrix (22) is the contribution of the air to the non-linear equation (19) to be solved where $[\mathbf{K}_{BEM}]$ is a full non-symmetric matrix linking together all the nodes belonging to $\partial\Omega_{FEM\cap BEM}$. This matrix has to be assembled with the conventional finite element tangent matrices using Newton-Raphson procedure:

$$[\mathbf{K}_{BEM}]=[\mathbf{T}].[\mathbf{G}]^{-1}.[\mathbf{H}] \quad (22)$$

3 ELECTROMAGNETISM AND MECHANICAL COUPLING

3.1 Mechanical modelling

As far EMF process is concerned, mechanical behaviour has to take into account high strain rates and the so-called Johnson-Cook model (23) is then used [6]. The model can also consider the influence of temperature, but this term is neglected for the reasons explained in the introduction. This assumption is confirmed by the thermal computation results presented in the next section.

$$\sigma=\left(A+B\left(\varepsilon_{eq}^{p}\right)^n\right)\left(1+C\ln\dot{\varepsilon}_{eq}^{*}\right)\left(1-T^{*m}\right) \quad (23)$$

with

$$\dot{\varepsilon}_{eq}^{*}=\frac{\dot{\varepsilon}_{eq}}{\dot{\varepsilon}_0} \text{ and } T^*=\frac{\theta-T_{ref}}{T_{melt}-T_{ref}}$$

$\dot{\varepsilon}_{eq}^{*}$ is the strain rate without dimension with $\dot{\varepsilon}_0$ usually set to $1.0s^{-1}$, T_{melt}, T_{ref} and θ represent respectively the melting temperature, a reference temperature like room temperature and the temperature in the structure.

3.2 Coupling procedure

The duration of the magnetic pulse is about several thousands µs. The coupling macro time step is usually set to 2 µs. First a magnetodynamic computation with SYSMAGNA® is done and the Laplace forces are calculated. These forces are then applied as loading conditions for the mechanical analysis performed with PAM-STAMP® or SYSTUS® at the end of which the geometry is updated to conduct a new electromagnetism computation. The coupling procedure iterates this way until the end of the process.

4 INDUSTRIAL APPLICATIONS

4.1 Deep drawing

In this example, the metal sheet is initially stamped

and the final shape is done using EMF process for which energy is provided by a coil inserted in the punch. Figure 2 illustrates the temperature field which maximal increase is 34°C at the end of the process. This temperature rise is only due to Joule effects under adiabatic conditions. Conduction has not time to operate as the process is too fast.

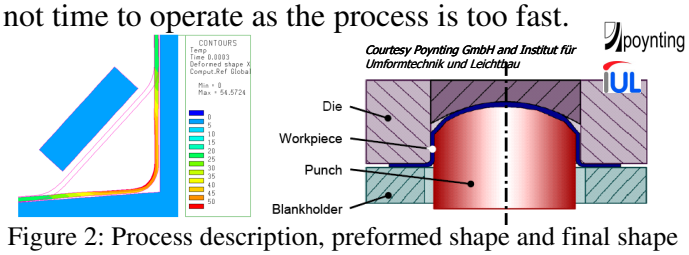

Figure 2: Process description, preformed shape and final shape with temperature field

4.2 Car door handle

This paragraph highlights all the technical functionalities of the software used to model the electromagnetic forming process. Indeed the proposed validation industrial example is non-rotationally symmetric and a die is required to accurately obtain the final deformed shape. The die is oval as shown in figure 3 and the coil is designed according this shape.

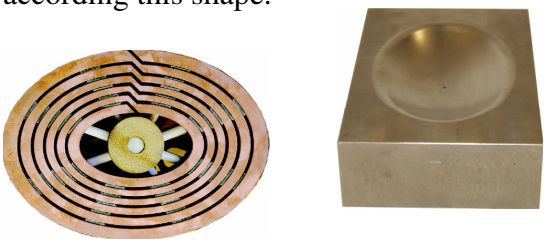

Figure 3: Coil and die geometry

The sheet is made of aluminium alloy. Two charging energies were tested for this component. With a charging energy of about 2100 J, the required deformed shape is not obtained. So, the comparison between experiments and calculations focuses on the process performed with a lower energy set to 1200 J. In this case the final geometry perfectly fits the die. Numerically, the results correlate with experiments as shown in figure 4.

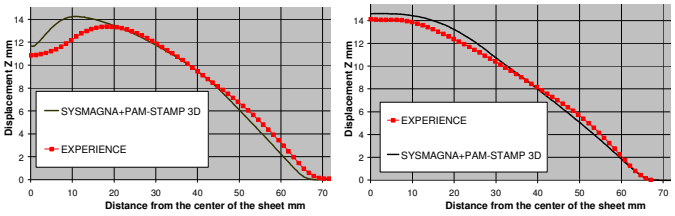

Figure 4: Displacements at the end of the process along the major axis for two charging energies.

5 CONCLUSIONS

The efficiency of the fully 3D coupled numerical modelling of electroforming process for virtual testing had been demonstrated. Indeed, experiments and computations correlate each other what is validating the assumption made on temperature effect. If boundary element method makes the work easier in this case, it generally also leads to higher CPU costs directly related to the number of nodes on the boundary. Finally, concerning tube forming, the advantage of 3D analysis compared with 2D ones is the ability to predict wrinkling effect due to thinning or non-perfect round shape.

REFERENCES

1. V. Psyk, C. Beerwald, M. Kleiner, M. Beerwald, A. Henselek, Use of electromagnetic forming in process combination for the production of automotive part, In: *Proceedings of the 2nd European Pulser Power Symposium*, Hamburg, Germany (2005).
2. J.-L. Coulomb, Analyse tridimensionnelle des champs électriques et magnétiques par la méthode des éléments finis, PhD thesis, Thèse d'Etat, (1981).
3. R. Pascal, P. Conraux, J.M. Bergheau, Coupling between finite elements and boundary elements for the numerical simulation of induction heating processes using an harmonic balance method, In: *IEEE Transactions on Magnetics, special CEFC issue*, 39 (3), (2003) 1535-1538.
4. J.M. Bergheau, Ph. Conraux, FEM-BEM coupling for the modelling of induction heating processes including moving parts, In: *Proceedings of the 1st International Conference On Thermal Process Modelling and Computer Simulation, Journal Of Shanghai Jiaotong University*, E5 (1), (2000) 91-99.
5. Ph. Conraux, M. Pignol, V. Robin, J.M. Bergheau, 3D finite element modelling of electromagnetic forming processes, In: *Proceedings of the 2nd International Conference on High Speed Forming*, Dortmund, Germany (2006) 73-82.
6. G. R. Johnson, W. H. Cook, A constitutive model and data for metals subjected to large strains, high strain rates and high temperature, In: *Proceedings of the 7th International Symposium on Ballistic*, (1983) 541-547.